Georisk
Vol. 5, Nos. 3–4, September–December 2011, 218–228

Taylor & Francis
Taylor & Francis Group

Load and resistance factor design (LRFD) calibration for steel grid reinforced soil walls

Richard J. Bathurst[a]*, Bingquan Huang[b] and Tony M. Allen[c]

[a]*GeoEngineering Centre at Queen's-RMC, Department of Civil Engineering, 13 General Crerar, Sawyer Building, Room 2414, Royal Military College of Canada, Kingston, Ontario, K7K 7B4, Canada;* [b]*GeoEngineering Centre at Queen's-RMC, Department of Civil Engineering, Queen's University Kingston, Ontario, Canada;* [c]*Washington State Department of Transportation State Materials Laboratory, Olympia, Washington, USA*

(Received 22 October 2009; final version received 24 April 2010)

This paper reports the results of load and resistance factor design (LRFD) calibration for pullout and yield limit states for steel grid reinforced soil walls owing to soil self-weight loading plus permanent uniform surcharge. The calibration method uses bias statistics to account for prediction accuracy of the underlying deterministic models for reinforcement load, pullout capacity and yield strength of the steel grids, and random variability in input parameters. A new revised pullout design model is proposed to improve pullout resistance prediction accuracy and to remove hidden dependency with calculated pullout resistance values. Load and resistance factors are proposed that give a uniform probability of failure of 1% for both pullout and yield limit states. The approach adopted in this paper has application to a wide variety of other reinforced soil wall technologies.

Keywords: retaining walls; steel grid reinforcement; load and resistance factor design; reliability; pullout; yield

Introduction

Limit states design, called load and resistance factor design (LRFD) in the USA, is now recommended in AASHTO (2007) for the design of foundations and earth retaining structures. Reinforced soil walls can be broadly classified into two categories: polymeric reinforced soil walls using relatively extensible geosynthetic products, and steel reinforced soil walls. In the latter category AASHTO (2007) and FHWA (2001) distinguish between walls constructed with steel strips and walls constructed with steel grids (bar mats and welded wire mesh). In the current AASHTO (2007) design guidance document, LRFD calibration for reinforced soil walls has been carried out by fitting to allowable stress design (ASD) together with accepted factors of safety for each limit state. This practice is undesirable since there is no guarantee that an acceptable target probability of failure is achieved and (or) load and resistance factors result in similar probabilities of failure for a suite of limit states. This paper is focused on LRFD calibration of reinforced steel grid walls using measured loads from instrumented field walls and resistance data for tensile rupture and pullout from independent laboratory tests.

The general approach used in this paper follows that described by Allen *et al.* (2005) and Bathurst *et al.* (2008a, 2009a). These papers also used data for steel grid reinforced soil walls as an example to demonstrate LRFD calibration concepts in the context of geotechnical earth structures. However, the current paper extends this earlier work by using a larger database of measured loads and a much larger database of pullout data from laboratory tests. In addition, the current study investigates LRFD calibration for the rupture (yield) limit state of the steel reinforcement. A novel approach illustrated in this paper is a technique to adjust the underlying deterministic model for pullout to simultaneously improve the prediction accuracy of the model and remove hidden dependency between resistance bias values and calculated (predicted) pullout capacity. The overall approach has application to the internal stability limit states design of a wide range of reinforced soil wall technologies provided that sufficient measured load data for walls under operational conditions is available together with resistance capacity data from physical testing.

Wall database

Tables 1 and 2 summarise the geometry and material properties for the steel grid walls used in this study. Five walls were built using bar mat and two walls using welded wire mesh. The walls are 4 to 18 m high

*Corresponding author. Email: bathurst-r@rmc.ca

ISSN 1749-9518 print/ISSN 1749-9526 online

DOI: 10.1080/17499518.2010.489828
http://www.informaworld.com

Table 1. Summary of steel grid wall cases [updated from Allen *et al.* (2001, 2004) and Bathurst *et al.* (2008a)].

Wall designation	Project date	Wall name	Reinforcement type	Number of data points[a]	Reference
BM1A,B	1981	Hayward wall, Section 1	Bar mat	8	Neely (1993)
BM2A,B	1981	Hayward wall, Section 2	Bar mat	6	Neely (1993)
BM3	1988	Algonquin wall (sand)	Bar mat	5	Christopher (1993)
BM4	1988	Algonquin wall (silt)	Bar mat	3	Christopher (1993)
BM5	1988	Cloverdale wall	Bar mat	5	Jackura (1988)
WW1	1985	Rainier Avenue wall	Welded wire	7	Anderson *et al.* (1987)
WW2	1991	Houston wall	Welded wire	8	Sampaco (1995)

Note: [a]Total number of data points (instrumented layers) n = 42.

with uniform surcharge loads less than 1.5 m equivalent soil height. The granular soil friction angle is between 35° and 43°. Reinforcement stiffness per unit width of wall is typically between 30 and 100 MN/m and global stiffness ranges from about 50 to 150 MN/m^2. The latter is a useful parameter to compare overall stiffness between walls that use different reinforcement types (e.g. steel and polymeric reinforced soil walls) and different numbers of layers (Allen *et al.* 2004, Bathurst *et al.* 2008b, 2009b). The vertical reinforcement spacing varied from 0.45 to 0.75 m. The reinforcement comes in prefabricated units (elements) with width between 0.15 and 1.2 m, but typically 0.4 to 0.6 m. The transverse member spacing is between 0.23 and 0.61 m. Bathurst *et al.* (2008a, 2009a) have used the same case study data, with the exception of case study WW2, in their example to illustrate the basic concepts of LRFD calibration. Using case study WW2 in the current paper increases the number of load data points available from 34 to 42.

Pullout and yield limit states

This paper is restricted to calibration of pullout and yield limit states for steel grid walls subjected to soil self-weight loading plus permanent uniform surcharge only. Hence, factored limit state functions have the form

$$\varphi R_n - \gamma_Q Q_n \geq 0 \quad (1)$$

Here, Q_n = nominal (specified) load; R_n = nominal (characteristic) resistance; γ_Q = load factor; and φ = resistance factor. Correct load and resistance factor calibration of a selected limit state must include bias statistics where bias is defined as the ratio of measured value to predicted (nominal) value. Bias statistics are influenced by model bias (i.e. intrinsic accuracy of the deterministic model representing the physics of the limit state under investigation), random variation in input parameter values, spatial variation in input values, quality of data and, consistency in interpretation of data when data are gathered from multiple sources (the typical case) (Allen *et al.* 2005). If the underlying deterministic model used to predict load or resistance capacity is accurate and other sources of randomness are small, then bias statistics have a mean value that is close to one and a small coefficient of variation. If the underlying deterministic models are poor, then adjustments to these models may be required in order to achieve sensible values for load and resistance factors (e.g. load factor values equal to or greater than one and resistance factor values equal to or less than one). Incorporating bias statistics into LRFD calibration and assuming only one load type, Equation (1) can be expressed as

$$\gamma_Q X_R \geq \varphi X_Q \quad (2)$$

Here, X_R = resistance bias computed as the ratio of measured resistance (R_m) to calculated (predicted) nominal resistance (R_n), and X_Q = load bias computed as the ratio of measured load (Q_m) to the calculated (predicted) nominal load (Q_n). For this transformation to be valid, bias values and corresponding predicted nominal values must be uncorrelated (i.e. no hidden dependencies). In this paper the predicted values for reinforcement load and pullout capacity are computed using the deterministic models (equations) recommended by AASHTO (2007) and FHWA (2001) and the specified yield tensile strength of the steel.

Load bias statistics

The maximum tensile load T_{max} in a reinforcement layer using the AASHTO Simplified Method (AASHTO 2002, 2007) is calculated using the following expression

$$T_{max} = S_v \sigma_v K_r \quad (3)$$

Here, S_v = vertical spacing of the reinforcement layer; σ_v = vertical earth pressure at the reinforcement depth; and K_r = lateral earth pressure coefficient. For steel grid walls, K_r varies from $2.5K_a$ to $1.2K_a$

Table 2. Summary of wall geometry and material properties for steel grid walls [updated from Allen *et al.* (2001, 2004) and Bathurst *et al.* (2008a)].

Wall designation	Wall height (m)	Surcharge condition	Soil friction angle[a] (°)	Vertical spacing, S_v (m)	Horizontal spacing of element[b], S_h (m)	Element width, b (m)	Coverage ratio, $R_c = b/S_h$	Transverse member spacing, S_t (m)	Reinforcement stiffness[c], J (MN/m)	Global stiffness[d] S_{global} (MN/m^2)
BM1A,B	6.1	2:1 slope, 25 kPa	41	0.60	1.05	0.60	0.57	0.60	66	109
BM2A,B	4.3	2:1 slope, 22 kPa	41	0.60	1.05	0.60	0.57	0.60	66	108
BM3	6.1	None	40	0.75	1.50	0.46	3.3	0.60	38	48
BM4	6.1	None	35	0.75	1.50	0.46	3.3	0.60	39	48
BM5	18.2	None	40	0.75	1.25	0.45–1.05	2.8–0.84	0.35–0.61	57–166	126
WW1	16.8	0.3 m soil surcharge	43	0.45	0.15	0.15	1.0	0.23	39–103	147
WW2	10.1	None	38	0.75	2.00	1.20	0.60	0.60	27–85	85

Notes: [a]Measured backfill peak triaxial or direct shear friction angle. [b]Centre-to-centre spacing of prefabricated group of longitudinal elements. [c]Stiffness J calculated assuming a steel modulus E = 200 GPa. The stiffness was computed as force per unit width of wall, based on geometry and horizontal spacing of the reinforcement (i.e. $J = EA/S_h$ where A is cross-sectional area of the reinforcement grid elements and S_h is centre-to-centre horizontal spacing). [d]Global wall stiffness $S_{global} = \Sigma J/H$.

at the top of the wall to a depth of 6 m and remains constant thereafter (Figure 1). Here, K_a is the active lateral earth pressure coefficient, which is a function of the peak soil friction angle ϕ. According to AASHTO, the friction angle is capped at $\phi \leq 40^\circ$. AASHTO (2007) makes no distinction between bar mat and welded wire walls. These two criteria are preserved in the current study. Recently released AASHTO (2009) interims propose that the maximum value of K_r be restricted to $1.7K_a$ for the pullout limit state only. The implication of this criterion to LRFD design using the recommendations in the current study are briefly reviewed at the end of the paper.

Figure 2(a) shows a plot of measured versus calculated (predicted) loads. The visual impression is that measured loads generally increase with calculated loads but there appear to be more data points below the 1:1 correspondence line than above. This is confirmed quantitatively by computing the mean of

Figure 1. Coefficient of earth pressure for calculating maximum reinforcement loads in steel grid reinforced soil walls using Simplified Method (AASHTO 2002, 2007). Note: H = height of wall.

load bias values where bias value is the ratio of measured to calculated load. This computation gives $\mu_Q = 0.89$ meaning that measured loads are about 10% lower than the calculated values *on average*. This is a conservative (safe) result for conventional ASD. Another visual observation is that the data for bar mat and welded wire walls are equally distributed. As a further check, the mean and COV of the bias values for each population were computed and shown to be close to the bias values for the entire dataset. Hence, welded wire and bar mat bias data are not treated separately in this investigation.

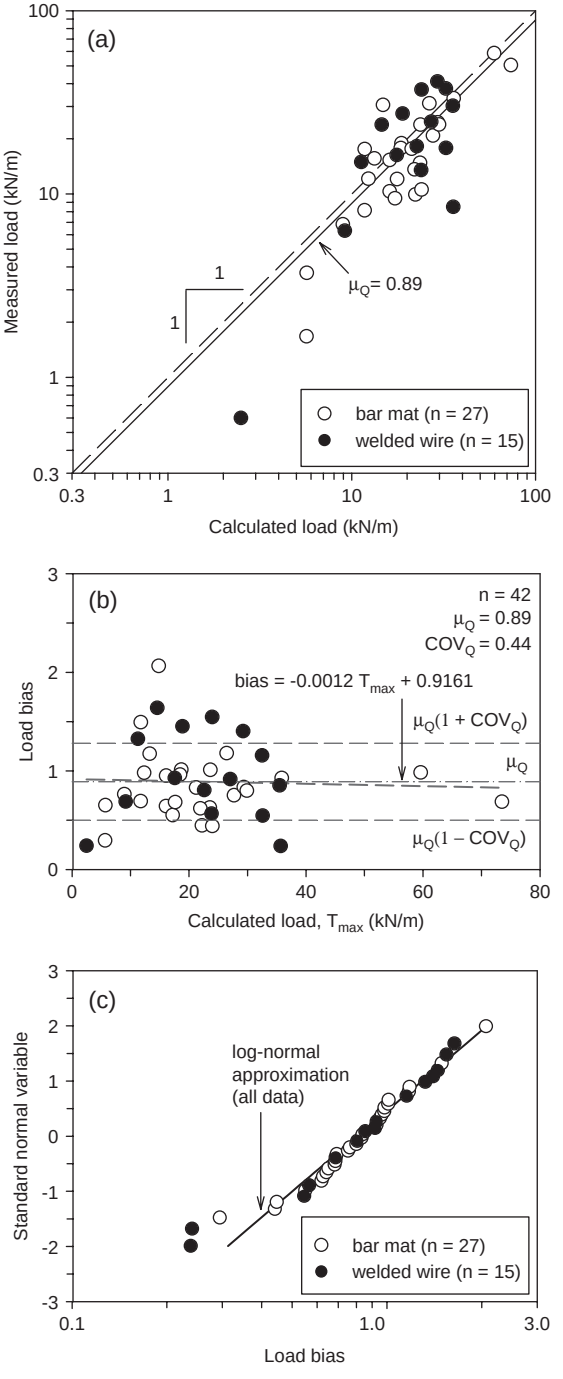

Figure 2. Steel grid walls: (a) measured versus predicted loads; (b) load bias versus calculated load; (c) CDF plot of load bias values.

It may be tempting to correct the load model by decreasing predicted loads by 10%. This can be done by shifting the design curve to the left in Figure 1 (i.e. multiplying by a correction factor of 0.90). However, because this correction would be applied to the entire range of calculated load values T_{max}, it is more convenient to leave the load model as is and effectively include the correction in the final choice of load factor as described in the next section.

Figure 2(b) shows bias values plotted against calculated loads. The linear regression line fitted to all data is visually very close to the horizontal line (mean of the entire data set) suggesting that there is no hidden dependency of bias values on calculated loads. As a quantitative check the 95% confidence interval on the slope of the regressed line (Draper and Smith 1981) was computed and shown to bracket zero. This confirms that at a level of significance $\alpha = 5\%$, bias values are independent of calculated loads and hence no adjustment to the load model is required (i.e. a horizontal line fit to the data is sufficiently accurate). This approximation also means the data do not need to be parsed into subsets based on calculated load ranges and different mean and COV values assigned to each group. Bathurst *et al.* (2008a) came to the same conclusion regarding non-dependency of load bias values using the Spearman correlation coefficient test on essentially the same data set. The cumulative distribution function (CDF) plot for the load data is presented in Figure 2(c). The predicted log-normal distribution fits most of the data reasonably well. The data for bar mat and welded wire walls are visually equally distributed. There is a visually poor fit at the lower tail that is exaggerated using a log-normal CDF plot, but this is not a practical concern since there is a good match at the upper tail. It is the fit to the upper tail of load bias values that is important for LRFD calibration as noted by Allen *et al.* (2005) and Bathurst *et al.* (2008a).

Load factor for steel grid walls

Figure 3 shows that 30% of the load bias values are greater than one (see cumulative distribution plot for unfactored load data). In LRFD calibration it is desirable to select a load factor that when multiplied against calculated (nominal) load increases the design load to an acceptable value (i.e. shifts distribution to the left by a satisfactory amount). In USA design codes the load factor for soil self-weight plus

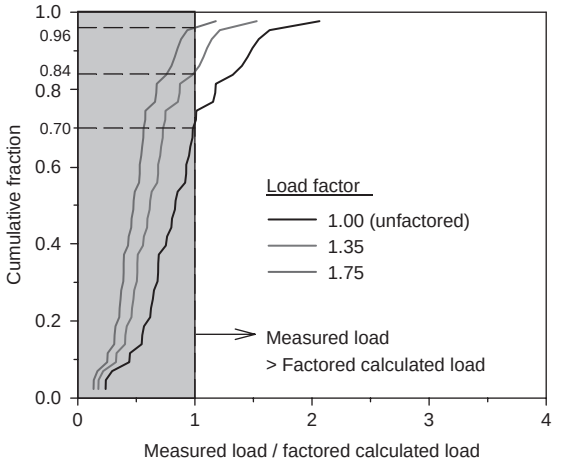

Figure 3. Influence of load factor on probability of exceeding measured loads for steel strip walls.

permanent uniform surcharge is called the vertical earth pressure load factor. Bathurst *et al.* (2008a) proposed a load factor of $\gamma_Q = 1.75$ for steel grid walls based on n = 34 (original) data points. In the current investigation, this value of the load factor applied to $n = 42$ data points gives a probability of exceedance of 4% (Figure 3). This value is close to the value of 3% that was assumed as a starting point during the development of the Canadian Highway Bridge Design Code (CSA 2006) and AASHTO (2007) for limit states design of superstructure elements in bridge structures (Nowak 1999; Nowak and Collins 2000). The AASHTO (2007) design code recommends a load factor of $\gamma_Q = 1.35$ which, if adopted here, results in 16% of measured loads being higher than calculated (predicted) values. However, the value of 1.35 is attractive because it is a value that is already in the AASHTO design code. The primary objective of LRFD calibration is to achieve a uniform target probability of failure for a set of limit states. The results of calculations presented later show that this objective can be met using $\gamma_Q = 1.35$. The results of using different load factors on probability of failure and calculation of resistance factors for pullout and yield limit states are also examined later.

Resistance bias statistics

Pullout capacity

According to AASHTO (2002, 2007) and FHWA (2001) the pullout capacity of a steel grid reinforcement layer can be calculated as

$$P_c = 2F^* L_e R_c \sigma_v \quad (4)$$

where, P_c = pullout capacity (kN/m); L_e = anchorage length (m); R_c = coverage ratio (b/S_h); σ_v = vertical stress (kPa); and F^* = dimensionless pullout resistance factor. The reinforcement may be discontinuous in the horizontal direction with elements (panels) of width b placed at centre-to-centre spacing S_h. The calculation of pullout capacity is on a unit running length of wall basis consistent with reinforcement load (T_{max}) dimensions (e.g. kN/m).

The pullout resistance bias values were calculated using the default F* values specified in current AASHTO and FHWA design codes using the design chart reproduced in Figure 4. The default F* value is a function of the transverse member thickness (diameter) t and transverse spacing S_t. The maximum F* value (= $20t/S_t$) occurs at the backfill surface and decreases linearly to $10t/S_t$ at a depth of 6 m, remaining constant thereafter.

The steel grid pullout data were taken from a database reported by Allen *et al.* (2001) (total of 41 tests) and data collected by the senior writer (an additional 29 tests). The specimens were manufactured with transverse bars of thickness (diameter) t = 6 to 13 mm and transverse spacing $S_t = 0.23$ to 0.61 m. Tests were carried out in laboratory pullout boxes together with granular soils.

Figure 5(a) shows measured versus predicted (calculated) pullout capacity values for steel grid data. Measured pullout capacity generally increases with predicted values indicating that the underlying deterministic model does well capturing the trend in

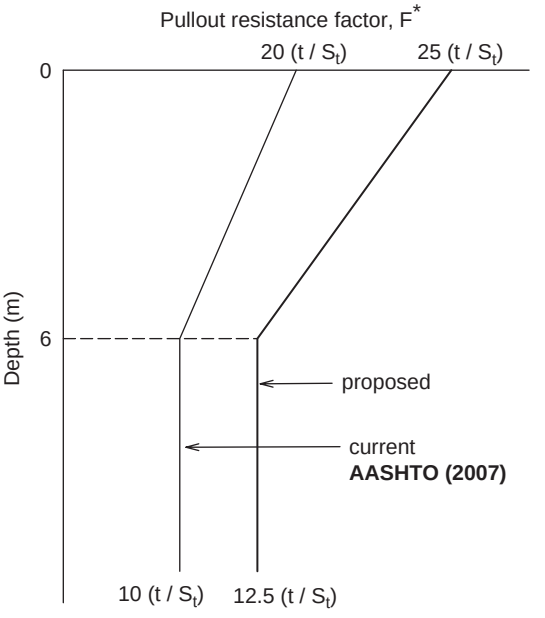

Figure 4. Current AASHTO (2007) and proposed default pullout resistance factor values for steel grid reinforcement materials.
Note: For proposed new model, if $P_c > 100$ kN/m then multiple P_c by 0.8.

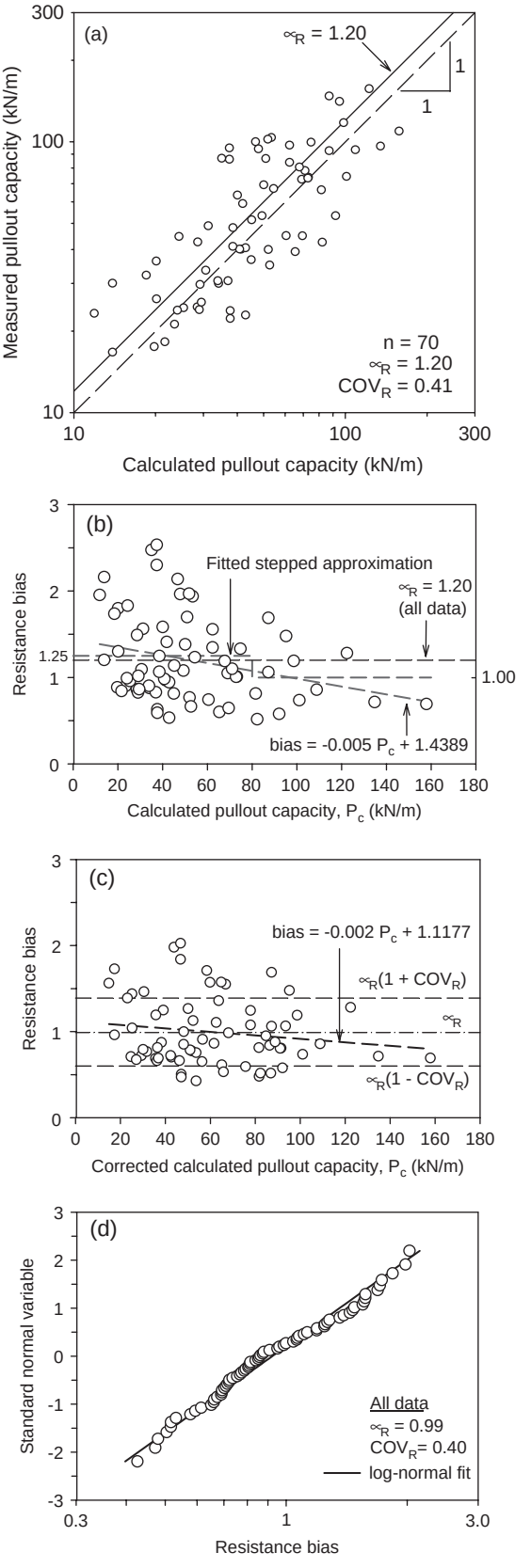

Figure 5 (*Continued*)

the data. However, the visual distribution suggests that the majority of the data points fall above the 1:1 correspondence line. This is confirmed by the average of bias values which is computed as $\mu_R = 1.20$ and used to plot the solid diagonal line in the figure. This means that the pullout model is conservatively safe *on average* for conventional factor of safety design. However, an over-estimation of pullout resistance by 20% is less desirable for LRFD calibration. Figure 5(b) shows resistance bias data plotted against calculated (predicted) values. The horizontal line corresponds to the mean bias value for the entire data set ($\mu_R = 1.20$). The data show what appears to be a visual dependency of resistance bias values with calculated pullout capacity values. A zero-slope test on all data confirms quantitatively that this is the case: specifically, the 95% confidence limits on the slope of the regressed linear line (sloped dashed line in the figure) are -0.009 and -0.001. Hence, a line with zero slope (no dependency) cannot be assumed to apply to this data at a level of significance $\alpha = 5\%$.

The strategy adopted here is to improve the pullout model with respect to the mean of bias values and dependency by parsing the data into two groups. The breakpoint was determined using the SOLVER optimisation utility in Excel with the objective function (sum of the squares of the differences) minimised and constrained to a stepped function as illustrated in Figure 5(b). The solution was adjusted slightly to give convenient constant values of 1.25 and 1.00 about the breakpoint at $P_c = 80$ kN/m. A practical implication of this observation is that the underlying default model is accurate *on average* for pullout capacity values greater than 80 kN/m using Equation (4) but is conservative (safe) for pullout capacity predictions less than this value (most of the data set). This deficiency in the pullout model can be corrected by multiplying calculated pullout values (Equation (4)) by a factor of 1.25 when $P_c \leq 80$ kN/m. Corrected bias values are re-plotted in Figure 5(c). The zero-slope test applied to the fitted linear line in the plot has a zero slope at a level of significance of 5%. A practical method for the design engineer to perform the same correction is to use the proposed F* design chart in Figure 4. Here the current AASHTO design curve has been multiplied by a factor of 1.25. However, a second correction is required for $P_c >$ 100 kN/m. These values must be multiplied by a factor of 0.8 to match the corrected bias values

Figure 5. Pullout resistance data: (a) measured versus calculated pullout capacity; (b) resistance bias values versus calculated pullout capacity; (c) resistance bias values versus corrected calculated pullout capacity; (d) CDF plot for corrected bias data.

corresponding to $P_c > 80$ kN/m plotted in Figure 5(c). Fortunately this correction is required for only about 17% of the pullout data points in this study. In practice, this correction would likely apply only to reinforcement layers at depths where pullout capacity does not control design.

The CDF for the corrected bias data is plotted in Figure 5(d). The mean and coefficient of variation of the corrected bias values are now 0.99 and 0.40, respectively. The log-normal approximation to the corrected bias data is a good fit over the entire data set and there is no need to perform a separate best fit to the lower tail. Furthermore, there is no longer the requirement to assign different mean and COV values to different ranges of calculated pullout load as was done by Bathurst *et al.* (2008a). This greatly simplifies LRFD calibration and the implementation of the method for the design engineer.

Rupture (yield) strength

A total of 22 tensile test results for rupture of steel grid materials were provided by one manufacturer. AASHTO (2007) uses the yield of the steel reinforcement ($f_y = 450$ MPa) as the nominal resistance value but these data were not available. Nevertheless, similar test data for steel strip reinforcement showed that the bias statistics are practically identical using rupture or yield strength measurements. Therefore, the statistical treatment of the steel grid rupture data is also considered applicable to yield of steel grids. Bias values were calculated as the ratio of measured to nominal (rupture) strength. The data are plotted as a CDF in Figure 6. The mean of the bias values is $\mu_R = 1.13$ based on all data. As may be expected for this manufactured material, the spread in bias values is very small ($COV_R = 0.08$) and very much less than for pullout bias statistics. Bias statistics for steel rupture reported here are very similar to yield bias values for concrete reinforcing steel reported by Nowak and Szerszen (2003).

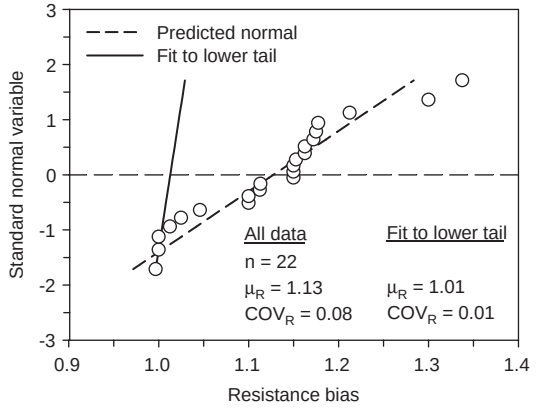

Figure 6. CDF plots for steel rupture strength bias values.

The predicted normal and log-normal distributions for the entire bias data are very close and a normal distribution can be assumed to be satisfactory. For such a narrow spread in the data, potential dependency of the type investigated earlier is not a concern.

It can be noted that there are no data points with bias values less than one. This is because the data are from production control records. Consequently, batches were rejected that had specimen strength values less than the nominal specified rupture value. Similar CDF plots with increased steepness at the truncated end for tensile yield and break of steel bars or strands used to reinforce concrete have been reported by Nowak and Szerszen (2003). A best fit to lower tail is shown in Figure 6 since it is the overlap of the lower tail of the resistance bias data with the upper tail of the load bias data that is most important for the calculation of probability of failure. The increase in steepness of the CDF plot for yield strength bias values has also been noted by the writers using production quality control data for steel strip reinforcement. These data give very similar bias mean and COV values for best fit to lower tail as the steel grid data in the current study. The result of using approximations to the entire data set and the fitted tail is demonstrated later in the paper.

Calibration results

In the LRFD calibrations to follow, the target probability of failure (P_f) is taken as 1 in 100 for reinforced soil walls as recommended by Allen *et al.* (2005) and Bathurst *et al.* (2008a). This corresponds to a reliability index value $\beta = 2.33$. The target probability may appear low but reinforced soil walls are highly strength-redundant systems. Hence, failure of one reinforcement layer will lead to load shedding to the other reinforcement layers without collapse of the structure. The same probability of failure ($P_f = 1\%$) and corresponding $\beta = 2.33$ value has been recommended for pile groups where failure of one pile in a group will lead to load shedding to other piles in the group without collapse of the group (system) (Paikowsky 2004).

Computed resistance factors using three assumed load factors and bias statistics for load and resistance data are summarised in Table 3. Monte Carlo simulations using an Excel spreadsheet (Allen *et al.* 2005; Bathurst *et al.* 2008a) were used to find the resistance factor in Equation (2) for each prescribed load factor and target $\beta = 2.33$. However, closed-form solutions reported by Bathurst *et al.* (2008a) also gave the same values within ± 0.01.

Table 3. Computed pullout and yield resistance factors (φ) for steel grid soil reinforced soil walls ($\beta = 2.33$, $P_f = 1\%$).

		Load bias values		Resistance bias values*				Resistance factor, φ	
		Fit to all data		Fit to all data		Fit to lower tail			
Limit state	Load factor, γ_Q	Mean μ_Q	COV_Q	Mean μ_R	COV_R	Mean μ_R	COV_R	Fit to all resistance data	Fit to resistance tail
Pullout	1.35							0.40	0.40**
	1.5	0.89	0.44	0.99	0.40	0.99	0.40	0.45	0.45
	1.75							0.52	0.52
Yield	1.35							0.69	0.64***
	1.5	0.89	0.44	1.13	0.08	1.01	0.01	0.77	0.70
	1.75							0.89	0.82

Notes: *Corrected resistance values using modified model for pullout capacity (Figure 4); **use 0.40 for design; ***use 0.65 for design.

The computed resistance factors for pullout range from 0.40 to 0.52. A value of $\varphi = 0.40$ is selected matching the load factor $\gamma_Q = 1.35$ recommended by AASHTO (2007). The same code recommends $\varphi = 0.90$, which is much higher. However, recall that the current pullout model under-estimates pullout capacity and the new recommended value ($\varphi = 0.40$) is developed from bias statistics using a more accurate pullout model. Yield limit state resistance factors vary with choice of resistance bias statistics from 0.64 to 0.89. A value of $\varphi = 0.65$ using best-fit-to-tail is judged to be a reasonable choice matching $\gamma_Q = 1.35$ and is also the value currently recommended in the AASHTO (2007) design code. The recommended load and resistance factors give the same target probability of failure ($P_f = 1\%$) for both limit states. However, to achieve the target probability of failure of 1% for pullout, Equation (4) and F* using the proposed new design curve in Figure 4 are required.

Comparison with ASD past practice

It is useful to compare factors of safety used in ASD past practice to equivalent values using the results of LRFD calibration. For the case of a single load factor the predicted (design) factor of safety can be estimated as

$$FS = \frac{R_n}{Q_n} = \frac{\gamma_Q}{\varphi} \tag{5}$$

Column 7 in Table 4 shows recommended factors of safety of 2.08 and 1.5 for yield and pullout, respectively, based on ASD past practice (AASHTO 2002; FHWA 2001). To examine the influence of the proposed load and resistance factors on performance, the actual or *operational factor of safety* can be computed for each limit state using ASD past practice and LRFD. The operational factor of safety (OFS) is defined as the ratio of the measured resistance (R_m) to measured load (Q_m) and is calculated as follows

$$OFS = \frac{R_m}{Q_m} = \frac{R_n \mu_R}{Q_n \mu_Q} = FS \cdot \frac{\mu_R}{\mu_Q} = \frac{\gamma_Q}{\varphi} \cdot \frac{\mu_R}{\mu_Q} \tag{6}$$

The results of these calculations are summarised in Table 4. The table shows that operational factors of safety for pullout using ASD (column 8) are larger than design values (column 7). This is consistence with the opinion of experienced design engineers that past practice is conservatively safe (e.g. loads in steel reinforced soil walls are lower than predicted values and pullout capacities are greater than predicted). This conservativeness has also been shown quantitatively in Figure 2(a) and Figure 5(a) and (b).

Table 4 shows that the actual in-service factor of safety for pullout for the walls in the database is greater (column 2) using the proposed LRFD load and resistance factors and the revised pullout model than the operational factor of safety (column 8) using ASD. Not unexpectedly, the corresponding probability of failure using ASD is also larger ($P_f = 11\%$ versus 1%).

For the yield limit state, the operational factor of safety is 2.64 using LRFD and ASD (column 2 and column 8) but larger than the specified value of 2.08 (column 7) in current design codes. Furthermore, regardless of which method is used the probability of failure remains 1%. Hence, there are no practical benefits of LRFD over ASD past practice for this limit state if both methods give the same target probability of failure. This also demonstrates that the result of LRFD calibration for this limit state is consistent with ASD past practice.

An alternative appreciation of the link between past practice and selection of resistance factor can be referenced to the data in the middle of Table 4. The values of resistance factor shown in Column 4

are computed based on the current estimated operational factor of safety (Column 5 = Column 8) and the prescribed load factor of 1.35. In other words, if the objective is to select resistance factors to match operational factors of safety for past practice with γ_Q fixed at 1.35, then the values shown in Column 4 are required. However, the penalty is that there this is a large difference in the probability of failure for each limit state.

Finally it should be noted that loss of section due to corrosion has not been included in the calibrations reported here. Sacrificial thicknesses of steel reinforcement can be computed using recommendations reported by AASHTO (2007) and FHWA (2001).

Conclusions and practical implications

This paper reports the results of LRFD calibration for pullout and yield limit states for reinforced soil walls that use steel grids (welded wire and bar mat). Calibration is limited to the case of a single load contribution owing to soil self-weight plus permanent uniform surcharge. The approach uses a database of measured reinforcement loads from field-instrumented walls and laboratory pullout tests. An important feature of the calibration method is the use of bias statistics to account for prediction accuracy of the underlying deterministic models for reinforcement load, pullout capacity and yield strength of the steel grids, and random variability in input parameters. In order to improve the accuracy of the pullout model for design, a revised estimation of the pullout model resistance factor (F*) for steel grid reinforcement is proposed.

The advantages of the proposed pullout calculation approach and calibrated LRFD load and resistance factors are:

a) Hidden resistance dependency for the pullout limit state is reduced.
b) Comparison with allowable stress design (ASD) past practice shows that the operational factor of safety for pullout using the new LRFD-based approach gives a higher factor of safety, but a lower probability of failure.
c) Compared to ASD past practice and current LRFD codes there is less chance of a reinforcement layer being under-designed or over-designed with respect to pullout.
d) Recommended load and resistance factors correspond to a uniform probability of failure for both pullout and yield limit states which is a desirable criterion for any set of limit states.
e) The load factor for soil self-weight ($\gamma_Q = 1.35$) is the same value recommended in the current AASHTO (2007) design code.

A useful check on the practical implications of the proposed LRFD approach and ASD past practice is to compare the pullout lengths required for the same reinforcement layer elevations in the wall database using both methods. These calculations show that the LRFD method requires 1.9 times the reinforcement length using ASD (with a factor of safety 1.5). However, AASHTO (2002, 2007) and FHWA (2001) impose the empirical constraint that the reinforcement length to wall height must not be less than $L/H = 0.7$. If this is done the ASD calculations show that 90% of reinforcement layer lengths are controlled by this empirical criterion. The end result is that the average increase in reinforcement length using LRFD is only about 15% greater for those layers that are controlled by pullout capacity. From a practical point of view this is considered to be a negligible difference from ASD past practice.

The probability of failure of 1% and 11% for yield and pullout, respectively, based on ASD past practice appears large (Column 9 in Table 4). However, there is no evidence that 1 in 11 or even 1 in 100 of reinforcement elements failed in the case

Table 4. Comparison of operational factor of safety (OFS) and probability of failure (P_f) using proposed LRFD approach and ASD past practice.

	Proposed LRFD using $\gamma_Q = 1.35$			LRFD using $\gamma_Q = 1.35$ and φ required to match AASHTO (2007) ASD OFS			ASD using AASHTO (2007)		
Limit state	φ	OFS[a]	P_f (%)	φ[b]	OFS	P_f (%)	FS specified (FHWA 2001)	OFS[c]	P_f (%)***
Column →	1	2	3	4	5	6	7	8	9
Pullout	0.40	3.75	1	0.74	2.02	10	1.50*	2.02	11
Yield	0.65	2.64	1	0.65	2.64	1	2.08**	2.64	1

Notes: [a]$OFS = \frac{\gamma_Q}{\varphi}\frac{\mu_R}{\mu_Q}$ and bias statistics for entire data sets; [b]$\varphi = \frac{\gamma_Q}{OFS}\frac{\mu_R}{\mu_Q}$ and bias statistics for entire data sets; [c]$OFS = FS\cdot\frac{\mu_R}{\mu_Q}$ and bias statistics for entire data sets; *$FS = \gamma/\varphi = 1.35/0.9 = 1.5$; **$FS = \gamma/\varphi = 1.35/0.65 = 2.08$; ***using unmodified load and resistance models and ignoring hidden dependencies.

study database due to internal stability modes of failure. In fact all of the walls in the database performed well. Furthermore, there is a long history of excellent performance of these systems in the field. Explanations for this apparent contradiction are: (1) the as-built pullout lengths of most reinforcement layers in the wall database were greater than lengths required to satisfy ASD past practice with a factor of safety of 1.5, and; (2) all calculated tensile loads were less than the design tensile capacity using ASD with a factor of safety of 2.08.

It should be noted that the design chart (Figure 1) for steel grid reinforcement loads in the recently released AASHTO (2009) design code interims that supersede AASHTO (2007) has been changed. In AASHTO (2009) the maximum value for the ratio of K_r/K_a is restricted to 1.7 for pullout calculations and the maximum value of 2.5 is used only for the yield limit state. A reduction in load was justified based on measured loads for steel strip walls reported by Bathurst *et al*. (2009) that led to the hypothesis that for granular soils with high friction angles there may be locally elevated compaction-induced loads. While it is recognised that compaction stresses are not likely to cause a pullout failure, data used to generate load bias values and Figure 1 are not available to differentiate between the portion of tensile load due to compaction effects and the additional load due to soil self-weight. It is the load due to soil self-weight that can cause a pullout failure mode if pullout deformations are sufficiently large. In other words, compaction-induced tensile loads in the reinforcement do not propagate to the anchorage zone. Hence, if a wall is designed using the calibrated LRFD method described here and the design chart in Figure 1, the structure will be safer than the same wall designed using the same LRFD approach but with a maximum value of $K_r/K_a = 1.7$ rather than 2.5 in Figure 1.

If the LRFD approach described in this paper is used for design there are likely additional sources of safety that are not considered explicitly using the underlying deterministic models and assumptions. For example, most engineers select reinforcement bar mat or welded wire mesh elements from stock materials that have greater cross-sectional area than the most critical reinforcement layer. Furthermore, the steel reinforcement members have additional post-yield tensile capacity and these wall systems are highly strength redundant.

If the load and resistance factors proposed in this study are used for design, the engineer of record should ensure that the structure being designed falls within the envelope of material property parameters, wall geometry, foundation conditions, and loading matching the database from which measured load and resistance statistics have been developed.

Finally, the paper has focused on LRFD calibration for internal stability of steel grid reinforced soil walls. Nevertheless, the general approach is applicable to other reinforced soil wall technologies provided that sufficient measured load data for walls under operational conditions is available together with resistance capacity data from physical testing.

Acknowledgements

Financial support for this study was provided by the Natural Sciences and Engineering Research Council (NSERC) of Canada, grants from the Department of National Defence (Canada), the Ministry of Transportation of Ontario and the following US State Departments of Transportation: Alaska, Arizona, California, Colorado, Idaho, Minnesota, New York, North Dakota, Oregon, Utah, Washington and Wyoming.

References

Allen, T.M., Bathurst, R.J., Holtz, R.D., Lee, W.F. and Walters, D.L., 2004. A new working stress method for prediction of loads in steel reinforced soil walls. *ASCE Journal of Geotechnical and Geoenvironmental Engineering*, 130 (11), 1109–1120.

Allen, T., Christopher, B., Elias, V. and DeMaggio, J., 2001. *Development of the Simplified Method for internal stability*. Report WA-RD 513.1 July 2001. Washington, USA: Washington State Department of Transportation, Olympia.

Allen, T.M., Nowak, A.S. and Bathurst, R.J., 2005. *Calibration to determine load and resistance factors for geotechnical and structural design*. Circular E-C079, Washington, DC: Transportation Research Board, National Research Council.

American Association of State Highway and Transportation Officials (AASHTO). 2002. *Standard Specifications for Highway Bridges*. 17th edition. Washington, DC: AASHTO.

American Association of State Highway and Transportation Officials (AASHTO). 2007. *LRFD Bridge Design Specifications*. 4th edition. AASHTO: Washington, DC, USA.

American Association of State Highway and Transportation Officials (AASHTO). 2009 *Interims*. *LRFD Bridge Design Specifications*. 4th edition. AASHTO: Washington, DC, USA.

Anderson, L.R., Sharp, K.D. and Harding, O.T., 1987. Performance of a 50-foot high welded wire wall. In *Proceedings of Soil Improvement—A Ten Year Update*. *Geotechnical Special Publication* No. 12, J.P. Welsh, editor. Reston, VA: American Society of Civil Engineering, 280–308.

Bathurst, R.J., Allen, T.M. and Nowak, A.S., 2008a. Calibration concepts for load and resistance factor

design (LRFD) of reinforced soil walls. *Canadian Geotechnical Journal*, 45 (10), 1377–1392.

Bathurst, R.J., Huang, B. and Allen, T.M., 2009a. Limit states design concepts for reinforced soil walls in North America. *In*: Y. Honjo, M. Suzuki, T. Hara and F. Zhang, editors, *Proceedings of the 2nd International Symposium on Geotechnical Risk and Safety*. Gifu, Japan, 11–12 June. London: Taylor & Francis Group.

Bathurst, R.J., Miyata, Y., Nernheim, A. and Allen, T.M., 2008b. Refinement of K-stiffness method for geosynthetic reinforced soil walls. *Geosynthetics International*, 15 (4), 269–295.

Bathurst, R.J., Nernheim, A., Walters, D.L., Allen, T.M., Burgess, P. and Saunders, D., 2009b. Influence of reinforcement stiffness and compaction on the performance of four geosynthetic reinforced soil walls. *Geosynthetics International*, 16 (1), 43–59.

Bathurst, R.J., Nernheim, A. and Allen, T.M., 2009c. Predicted loads in steel reinforced soil walls using the AASHTO Simplified Method. *ASCE Journal of Geotechnical and Geoenvironmental Engineering*, 135 (2), 177–184.

CSA. 2006. Canadian highway bridge design code (CHBDC). CSA Standard S6-06. Toronto, Ontario: Canadian Standards Association (CSA).

Christopher, B.R. 1993. *Deformation response and wall stiffness in relation to reinforced soil wall design*. Thesis (PhD), Purdue University, West Lafayette, Indiana, USA.

Draper, N.R. and Smith, H., 1981. *Applied regression analysis*. 2nd edition. New York: John Wiley.

Federal Highway Administration (FHWA). 2001. Mechanically Stabilized Earth Walls and Reinforced Soil Slopes —Design and Construction Guidelines. *In*: V. Elias, B.R. Christopher and R.R. Berg, editors. *FHWA-NHI-00-043*. Washington, DC: Federal Highway Administration.

Jackura, K.A. 1988. *Performance of a 62-foot high soil reinforced wall in California's North Coast Range*. Internal Rep., CALTRANS, Division of New Technology and Research California, USA.

Neely, W.J. 1993. Field performance of a retained earth wall. Renforcement Des Sols: *Experimentations en Vraie Grandeur des Annees 80*. Paris: Presses de L'école Nationale des Ponts et Chaussees, 171–200.

Nowak, A.S. 1999. *Calibration of LRFD bridge design code*. NCHRP Report 368, National Cooperative Highway Research Program. Washington, DC: Transportation Research Board.

Nowak, A.S. and Collins, K.R., 2000. *Reliability of structures*. New York: McGraw Hill.

Nowak, A.S. and Szerszen, M., 2003. Calibration of design code for buildings (AC 318): Part 1 – Statistical models for resistance. *ACI Structural Journal*, 377–382.

Paikowsky, S.G. 2004. *Load and resistance factor design (LRFD) for deep foundations*. NCHRP Report 507, National Cooperative Highway Research Program. Washington, DC: Transportation Research Board.

Sampaco, C.L. 1995. *Behavior of welded wire mesh reinforced soil walls from field evaluation and finite element simulation*. Thesis (PhD), Utah State University, Logan, Utah, USA.